Chapter 12
Application to Underground LNG Storage

Eui-Seob Park, Yong-Bok Jung, Taek Kon Kim, and Baotang Shen

Abstract This chapter introduces the underground LNG storage technology which is superior in safety, economic and environmental aspects to a conventional above-ground and inground storage type and shows various results of the pilot test done for technical verification of the new storage method. We also show the results of applying the FRACOD analysis function developed to simulate the thermo-mechanical coupling behavior of the rock mass surrounding the storage cavern and the ice ring formation process due to the cryogenic LNG storage.

For the purpose of this publication, it presents recent developments of the thermal-mechanical coupling and ice swelling functions in FRACOD, a numerical code designed to predict rock fracturing processes in fractured rock masses. The new functions enable us to investigate the complicated response of an *in situ* rock mass to the excavation of LNG cavern and the storage of low-temperature LNG in a most realistic way.

Keywords Underground LNG storage · Rock cavern · Ice ring · Crack · Propagation · Toughness · Coupled behavior

E.-S. Park (✉) · Y.-B. Jung
KIGAM, Daejeon, Republic of Korea
e-mail: espark@kigam.re.kr; ybjung@kigam.re.kr

T. K. Kim
SK E&C, Seoul, Republic of Korea
e-mail: tkkim@sk.com

B. Shen
CSIRO Mineral Resources, Brisbane, Queensland, Australia

Shandong University of Science and Technology, Qingdao, China
e-mail: Baotang.Shen@csiro.au

B. Shen et al. (eds.), *Modelling Rock Fracturing Processes*,
https://doi.org/10.1007/978-3-030-35525-8_12

12.1 Introduction

Underground rock caverns have been commonly used and safely operated for many decades to store petroleum products such as crude oil, propane, and butane, either compressed or refrigerated. The underground storage is of particular interests in reducing the surface footprint and enhancing safety and security. It also reduces the visual impact of storage and is economically attractive.

However attempts to store Liquefied Natural Gas (LNG) in underground rock caverns with a similar approach have not been considered satisfactory due to the large boil-off gas rate and the low LNG temperature acting on the rock wall which is liable to generate cracks in the rock mass (Glamheden 2001).

One of the methods to prevent a hard rock mass from thermal cracking at LNG (Liquefied Natural Gas) boiling temperatures (−162 °C) is to locate the unlined storage cavern deep enough below the ground level so that the *in situ* stresses counterbalance the tensile stresses caused by the cooling. The necessary depth varies with rock types from 500 to 1000 m, which renders this unlined cavern storage concept very expensive. On the other hand, the storage of LNG in in-ground insulated tanks has proven to be reliable, though expensive, method (Amantini and Chanfreau 2004; Amantini et al. 2005).

A key issue of storing LNG in the caverns is to protect the host rock mass against extremely low temperature (e.g. −162 °C). One of the key technical challenges is to understand the behavior of the rock mass in the vicinity of the LNG cavern and hence take measures to prevent leakage caused by possible rock fracturing in response to the cooling of the rock mass. With the extremely low temperature of the LNG in the storage cavern, the sub-zero temperature will be induced in the surrounding rock mass, which may cause tensile stress due to thermo-mechanical effect and will also cause the formation of ice in pores and cracks of the saturated rock mass. Ice formation is likely to cause compressive stress in the rock mass due to its expansion in volume. The combined effect of rock cooling and ice swelling is complicated as cooling tends to create open fractures whereas ice swelling tends to cause compression. Understanding this effect is crucially important as it is related to the integrity of the surrounding rock mass for leakage prevention.

A new concept for storing LNG in a lined rock cavern has been developed to provide a safe and cost-effective solution and validated by the pilot LNG project. It consists of protecting the host rock against the extremely low temperature by insulation and providing a liquid and gas-tight liner. Moreover, the moderated and controlled freezing of groundwater in the surrounding rock mass contributes to creating an ice ring, acting as a secondary barrier against any possible leakage (Chung 2006). The main point of the new storage technology is to form an ice ring around the cavern with suitable thickness so that there is no groundwater in the rock near the cavern. If this fails, the groundwater present in the rock will turn into ice due to cryogenic storage, which will cause expansion pressure and adversely affect the storage system. So, thermal–mechanical integrity of rock mass and lining

system is a crucial factor in the construction and operation of the underground LNG storage facilities.

The thermal–mechanical coupling and ice swelling functions are developed in FRACOD, and coupled analyses have been carried out in order to simulate the fracture initiation and propagation of thermal fractures around the pilot LNG storage cavern. And the capability of FRACOD has been investigated by a comparison of numerical results with *in situ* measurement data. The new functions enable us to investigate the complicated response of the *in situ* rock mass to the excavation of LNG cavern and the storage of low-temperature LNG in a most realistic way.

12.2 Basic Concepts of LNG Storage in Underground Rock Caverns

The basic concept of LNG storage in membrane lined rock caverns is a combination of well-proven technologies and a new concept named "formation of ice ring" as shown in Fig. 12.1. The three basic concepts are described in detail below.

12.2.1 Underground Rock Cavern

The underground storage technology, which proved reliable, experienced a strong development related to its intrinsic qualities, but also on the innovations and technical progress from which it regularly profited. Especially underground storage facilities provide a lot of advantages as followings: no exposure to threats of natural disasters such as an earthquake, tsunami, and typhoon, and increased security against man-made disasters of fire, war and terrorism, and minimized land lease and environmental friendliness.

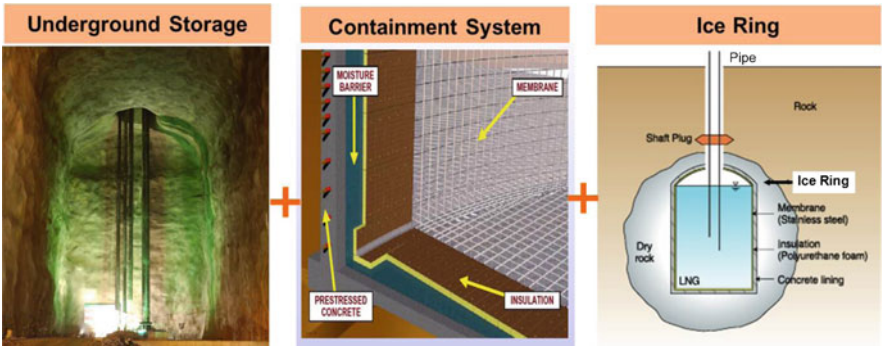

Fig. 12.1 Three basic concepts of the lined rock cavern system for storing LNG (Park et al. 2011)

Most of all, the major strength of underground storage is in its economic feasibility. As the economic feasibility of the underground storage is realized at large scales, the cavern geometry is optimized at the maximum possible cross-section with a sufficient degree of structural stability. Currently, large capacity of storage cavern units with more than several hundreds of thousands of cubic meters, for a broad range type of hydrocarbon products and crude oil, have been constructed and operated successfully, especially in Korea. And Korea has accumulated technical know-how in this field based on more than 30 years of experience in design, construction, and operation of underground storage facilities (Kim 2006).

12.2.2 Membrane Containment System

The membrane containment system has been successfully used in several LNG carriers and storage tanks. This membrane system provides the proper thermal protection for surrounding rock mass to prevent excessive stresses and crack formation and reduce the boil-off to the level of conventional LNG storage tanks. Also, it provides a liquid and gas tight liner using a corrugated stainless steel membrane fixed on insulating panels and a concrete lining. The thermal characteristics and thickness of the insulation are designed to obtain the minimum allowable temperature in the rock mass for the design life of the storage and a boil-off rate of less than 0.1% per day. The modular structure of the containment system makes it very flexible, which improves construction and adjusting to the cavern geometry. The thickness of the insulating panel can be adjusted to increase the thermal efficiency and the almost unstressed membrane allows very large-scale projects.

12.2.3 Ice Ring and Drainage System

The concept of ice ring is newly developed to solve the problems of the conventional storage method and plays a very important role in ensuring the integrity of the new storage system. In the case of groundwater intrusion into the containment system, the integrity of the containment system could be destroyed because of the volume expansion of the groundwater during the freezing process. So a new groundwater control system was introduced to drain the water around the cavern and prevent hydrostatic pressure acting against the containment system. And it can be used to balance the migration of the 0 °C -isotherm by applying water with a specific temperature for water infiltration. The groundwater drainage system is composed of a series of boreholes drilled from the surface and/or dedicated drainage galleries installed around the cavern (Fig. 12.2). Reduction of high water seepage by grouting in the cavern will generally be needed. This is achieved by systematic grouting works during excavation.

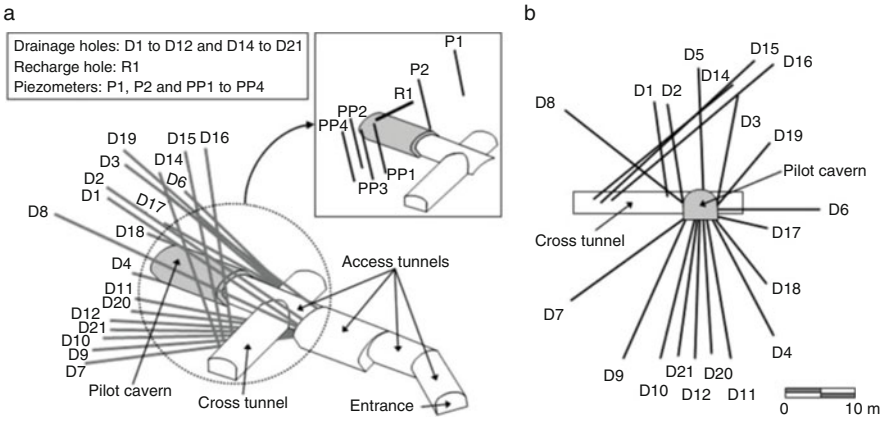

Fig. 12.2 Schematic diagram of the pilot cavern, (**a**) Oblique view of drainage holes (D series), recharge hole (R1), and piezometers (P and PP series) & (**b**) front view of drainage holes (Cha et al. 2007)

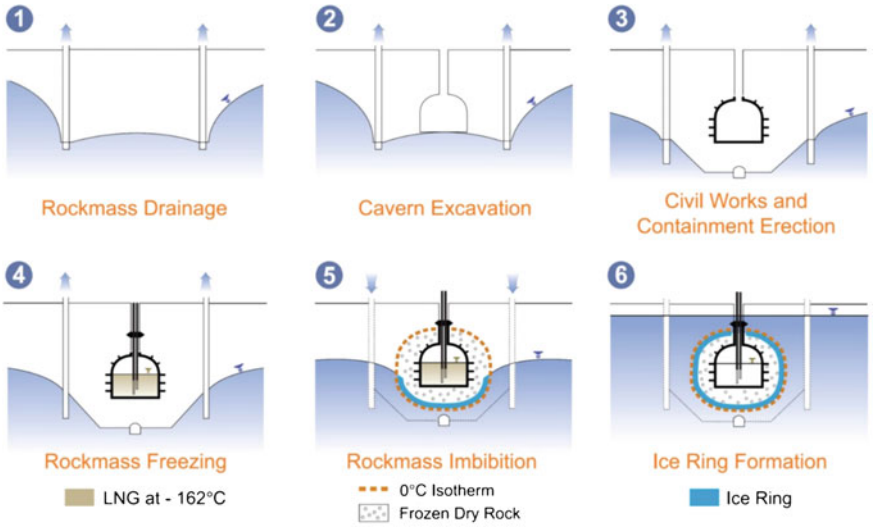

Fig. 12.3 Schematic diagram of the formation of ice ring (Park et al. 2011)

Although the ice ring is supposed to play an important part as a secondary barrier against leakage of stored LNG, the location, and thickness of the ice ring are important factors for the stable storage of LNG in a lined rock cavern. Formation of ice ring can be explained by each stage of construction of a lined rock cavern (Fig. 12.3).

Groundwater is temporarily removed from the rock surrounding the cavern during the first phase of construction. This preliminary de-saturation of the host

rock mass aims at preventing unacceptable hydrostatic pore pressure and ice formation behind the cavern lining.

After excavation of cavern and installation of containment system are completed, LNG will be stored in the cavern and then the cold front starts propagation from the cavern at the same time. When the cold front has advanced far enough from the cavern wall, drainage can be stopped to allow groundwater progressively to rise up and quickly form a thick ring of ice around the cavern. After the ice ring is completely formed, the operation of the drainage system is stopped. The drainage period during LNG storage will last several months or years, depending on the thermal properties of rock masses and hydro-geological characteristics on the site.

12.3 Mechanical Behavior of Rock Mass under Cryogenic Conditions

The concepts for underground gas storage differ from each other according to the confinement and sealing principle applied. A gas under atmospheric or low pressure can only be stored in a liquid state, thus applying refrigeration up to −160 °C. In this case, the emphasis is placed on thermal insulation and sealing for the liquid and/or the low-pressure vapor. The containment – as a structural element – is subjected to very little loading, due to low pressure (Kovári 1993).

In prior attempts of storing LNG in unlined rock caverns (Broms et al. 2001; Jacobsson 1977; Lasseter and Witherspoon 1974), the criterion is mainly concerned with the opening of existing natural fractures on the rock surface. Such opening may cause leakage of stored liquid gas through fractures, resulting in an excessive boil-off rate of gas and consequent failure of the storage. In case of lined rock cavern, since the containment system and concrete lining prevent the existing fractures from being in direct contact with the cryogenic liquefied gas, the opening of such fractures is allowed to some extent. Thus, the criteria for evaluating thermo-mechanical stability of lined rock cavern are concerned with the initiation of new fractures and propagation of existing fractures within the considered temperature range. While the criterion for preventing initiation of new fractures in the rock mass is based on conventional strength concept, propagation of the existing cracks and fractures should be dealt with fracture mechanics concept because the major factor for assessment of stability, in this case, is the stress concentration at the crack tip.

When such lined rock cavern is used for LNG storage, its thermo-mechanical stability depends on the initial in-situ rock stress (Phase I), stress concentrations in the vicinity of the cavern due to excavation (Phase II), and thermally-induced stress during operation of the cryogenic storage (Phase III) as illustrated in Fig. 12.4.

In Fig. 12.4, σ^{I}, σ^{II}, and σ^{III} denote in-situ rock stress field before excavation (σ_V^I, σ_H^I: vertical and horizontal stresses), redistributed stress field after excavation (σ_r^{II}, σ_θ^{II}: radial and tangential stresses) and thermally induced stress field during operation of cryogenic storage (σ_r^{III}, σ_θ^{III}: radial and tangential stresses), respectively. In prior

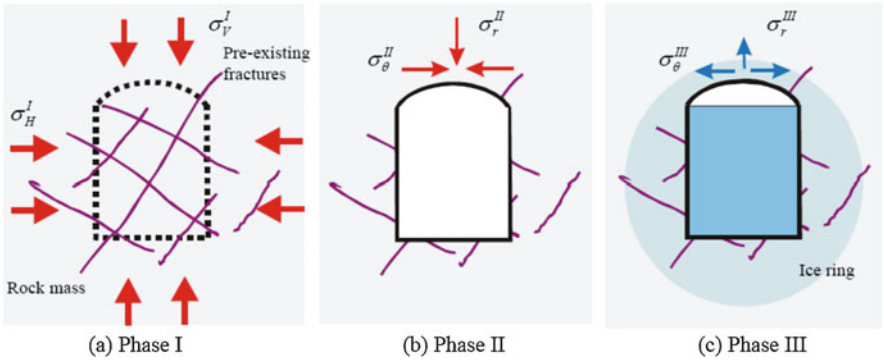

Fig. 12.4 Schematic diagram of involved stress fields in rock mass during the construction and operation of underground LNG storage cavern (Lee et al. 2006)

attempts of storing LNG in unlined rock cavern, the criterion is concerned with the opening of existing natural fractures on the rock surface. The temperature at which the opening of existing fractures occurs coincides with the point at which tangential component (σ_θ^{III}) of the induced thermal stress during phase III becomes zero, indicating the transition of the stress from compression to tension. At this temperature, the arching effect around the cavern disappears and the existing rock blocks become unstable (Lee et al. 2006).

The new criteria for evaluating the thermo-mechanical stability of lined rock cavern are concerned with both initiations of new fractures and propagation of existing fractures. Initiation and propagation of such fractures will cause instability of the rock mass around the cavern, and in extreme cases, it may accompany leakage of stored gas leading to the ultimate failure of the system.

Generally, new fractures are initiated when the tangential rock stress during phase III becomes tensile and exceeds the tensile strength of the rock. However, since the tensile strength of rock varies with temperature and the amount of thermal shock, such variation should be taken into account when establishing the criteria for preventing initiation of new fractures in the rock mass. The temperature at which new fractures are initiated can be obtained based on a theoretical approach, and it may be used as an evaluation criterion at the initial design stage.

Because the mechanism of fractures generation or extension in rock masses under LNG storage could be different due to pre-existing fractures and freezing of groundwater in fractures, each mechanism would be reviewed as followings.

12.3.1 Initiation of New Fractures Due to Cooling Down

It has been known that when a rock is cooled slowly, thermal cracks due to the difference of thermal expansion between components of rock are generated although a temperature gradient is not steep. Therefore a microfracture could be initiated when

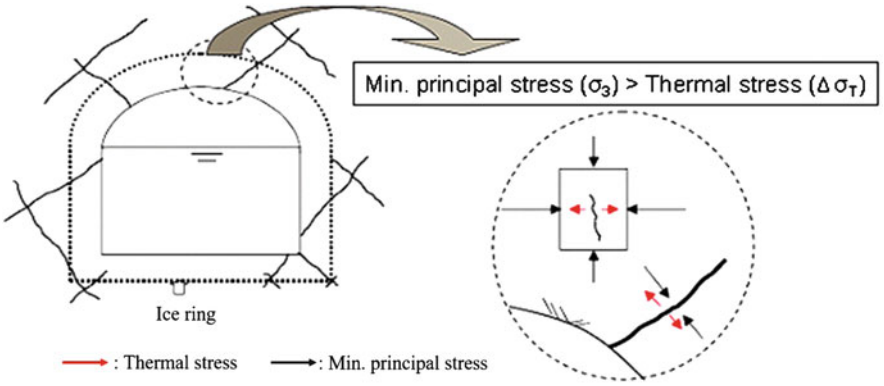

Fig. 12.5 The stable criterion for suppressing the initiation of a new fracture (Park 2006)

thermal stress exceeds the tensile strength of a rock. However, because there is an effect of compensating tensile stresses with thermal stresses when initial stresses (compression) are present, the fracture generations due to thermal shock would be suppressed.

According to Goodall (1989), a condition for a successful operation of chilled gas storage can be expressed below in Eq. 12.1.

$$\text{in situ stress} + \text{tensile strength} > \text{thermal stress} \tag{12.1}$$

If there is a significant internal storage pressure, this contributes to the right-hand side of the equation; however, in the case of chilled storage, the internal gas pressure (0.01–0.03 MPa) is very low and negligible in the above equation. In the same way, the hydraulic pressure caused by water curtains or the high groundwater act as a factor to reduce the in-situ stress values, in other words, it increases the likelihood of fracturing in the rock mass.

As shown in Fig. 12.5, the stable criterion for suppressing the initiation of new fractures is suggested that fractures are not initiated when the thermally induced stress due to cooling down is smaller than the minimum principal stress in surrounding rock mass.

In general, numerical simulations do not take into account the tensile strength of rock mass, so this criterion is considered somewhat conservative. Additional research is needed to verify and supplement the criteria.

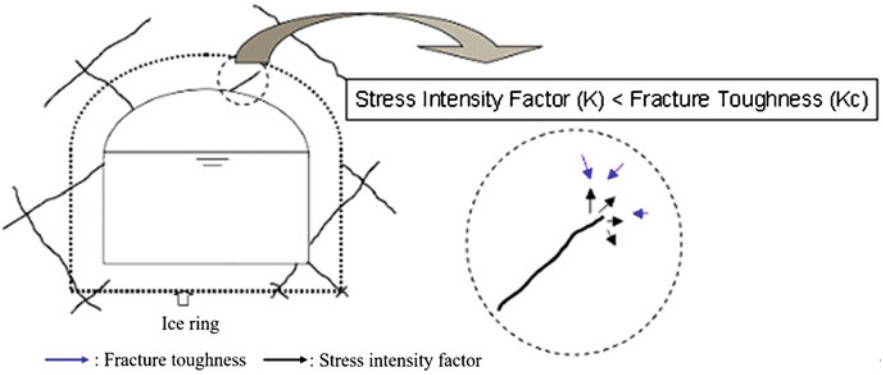

Fig. 12.6 The stable criterion of suppression of an existing fracture propagation (Park 2006)

12.3.2 Propagation of Existing Fractures Due to Cooling Down

It is defined in linear elastic fracture mechanics that fracture propagation occurs when stress intensity factor (K) at the crack tip is greater than or equal to the fracture toughness of material ($K \geq Kc$). It is well known that most works on fracture propagation in rock mass have been related to mechanical or hydraulic loads (Lee et al. 2006). Rahman et al. (2000) have evaluated the possibility of propagation of rock fractures subjected to internal fluid pressure under *in situ* rock stresses.

During the construction of caverns, the groundwater in the fractures of rock mass would be staying locally when drained unsuccessfully. In this case, the groundwater could be frozen during the operation of LNG storage and the frost heaving pressure that builds up due to phase change of water into ice acts in the opposite direction of excavation-induced stresses and stimulates fracture propagation as the temperature decreases.

If the fracture density of rock mass is high, many of the fractures intersect each other and form rock blocks. In this case, the local thermal stresses can be diminished by the relative movement of the blocks. Therefore, the fracture density of rock mass should be considered in the criterion for fracture propagation.

To derive a criterion for preventing fracture propagation in the rock mass, the effective stress intensity factor must be obtained in terms of effective stress components on the considered fracture plane. The propagation mechanism of an existing fracture could be explained through relations between stress intensity factor (K) and fracture toughness (Kc) at a crack tip as shown in Fig. 12.6.

12.4 Experiment of Pilot LNG Cavern

To validate the basic concept of underground LNG storage, A pilot LNG cavern was constructed by SKEC and KIGAM at Daejeon, Korea in 2003–2004 and comprehensive thermal, hydrological and mechanical tests were performed (Amantini and Chanfreau 2004, Amantini et al. 2005, Park et al. 2007a, b, 2010).

The key factors considered during design, construction and operation stage of underground LNG storage are as followings:

Physical and mechanical properties of rock mass at a low temperature
Occurrence and propagation of fractures
Stress change by induced thermal stress
Calculation of heat flux (conduction + convection)
Convection rate in rock joint
Monitoring of thermal stress and displacement
Monitoring of temperature change
Resistance to thermal shock during cooling down
Frost heaving at low depth

The pilot cavern is 4.2 m wide and 4.2 m high, and it was excavated at a depth of about 22 m below the ground surface. The base rock consists of Jurassic biotitic granite intruding Pre-Cambrian gneiss, which has an RQD of 80–86 and the most frequent Q-value of 12.5. The Q-value requires no supports or minor unreinforced shotcrete (about 40 mm) and bolt according to support categories of Q-system. Therefore, it is proper to adopt rock bolting to stabilize the main fractures of the existing cavern and ensure the stability of the possible fracture position.

The cavern had a concrete lining of 0.2 m thickness followed by a 0.1 m thick polyurethane (PU) foam panels for thermal insulation. The internal dimensions of the completed pilot plant have a sectional dimension of 3.5 m × 3.5 m, a length of 10 m, amounting to a working volume of 110 m^3 (Fig. 12.7).

Fig. 12.7 A birds-eye-view and a cross-section of the pilot cavern (Park et al. 2010)

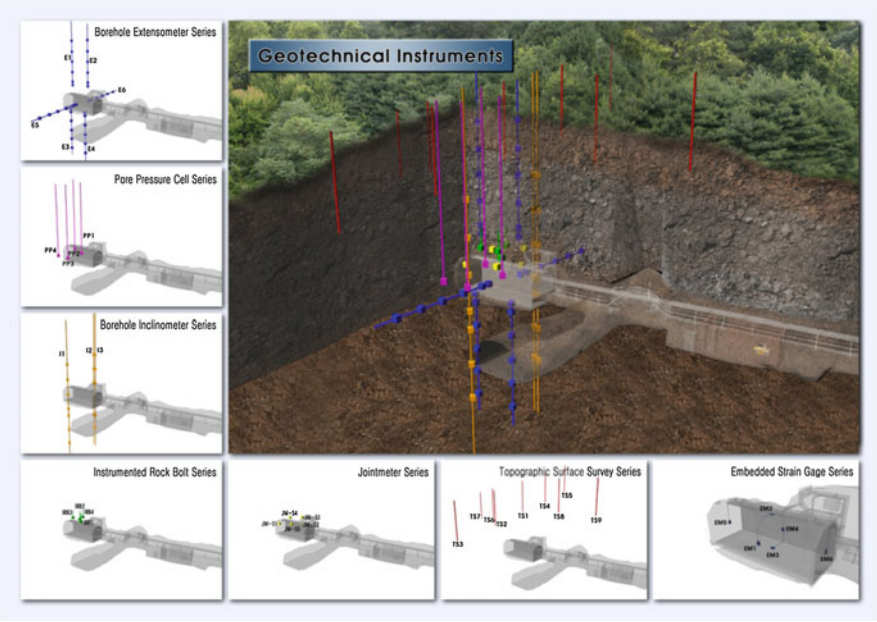

Fig. 12.8 Illustration of the pilot LNG cavern at Daejeon and the location of geotechnical instruments (Jung et al. 2014)

The experiment started in January 2004 and the pilot cavern was filled with liquefied nitrogen at a temperature of −196 °C to the height of about 2.5 m for about 6 months. The top part of the pilot LNG cavern was a boil-off gas at a temperature of −40 °C. During the field experiment of the pilot LNG storage cavern, a lot of instruments were installed in the surrounding rock mass to survey both operation parameters and thermo-hydro-mechanical behavior of rock masses (Fig. 12.8).

This pilot experiment provided invaluable field data assisting the understanding of rock mass response to the LNG storage, and many studies have since been carried out to analyze the information and model the coupled thermal-hydraulic-mechanical behavior of the underground storage cavern and its surrounding rock mass (Yi et al. 2005; Cha et al. 2007; Jung et al. 2011).

Many reports and articles on the pilot LNG storage cavern regarding operation, survey, geophysical and geotechnical monitoring, field experiments with numerical modeling, and so on have been published (Cha et al. 2006, 2007; KIGAM 2003, 2004, 2005, 2006; Kim et al. 2007; Lee et al. 2003; Park et al. 2007a, b, 2010; Yi et al. 2005).

12.5 Coupling Between Rock Fracturing and Thermal Process in FRACOD

In a fractured rock mass, rock fracturing, fluid flow, and rock temperature change are closely correlated (Fig. 12.9). Rock fractures will enhance the fluid flow by creating new flow channels, whereas the fluid pressure may stimulate fracture growth. A temperature change will result in thermal stress in the rock mass which could lead to fracture propagation. Coupling between these processes is necessary in order to study the industrial issues mentioned previously.

To deepen the knowledge on the above-mentioned issues and to understand the coupled F–T–H processes in rocks on an engineering scale, the recent development of FRACOD has been focused on the coupled processes between rock fracturing and thermal and hydraulic processes. This section summarizes the theoretical background and numerical considerations of the coupled F–T function and the related ice swelling function in FRACOD.

The coupling between rock fracturing and thermal processes is a one-way coupling with stresses dependent on the temperature field following thermo-elasticity principles. As the DD method used in FRACOD is an indirect boundary element method, an indirect method is also used to simulate the temperature distribution and thermal stresses due to internal and boundary heat sources. With this method, fictitious heat sources with unknown strength over the boundary of the domain are used, and it is, therefore, easier to consider the problem with internal heat sources (Shen 2014).

Also, the new function in FRACOD was designed to simulate the ice swelling pressure in explicit rock fractures. Due to the current limitation of FRACOD in simulating the porous flow, at this stage, we only consider the swelling pressure in rock fractures. Water may exist in three different phases in a rock mass at low temperature (Fig. 12.10):

- Liquid phase (water) – at a temperature normally >0 °C
- Transient phase (water and ice) – at a temperature from −2.5 °C to 0 °C
- Solid phase (ice) – at a temperature < 2.5 °C

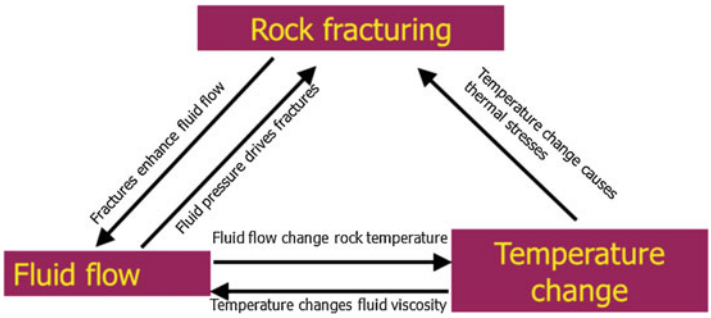

Fig. 12.9 Interaction between rock fracturing and fluid flow and rock temperature changes (Shen 2014)

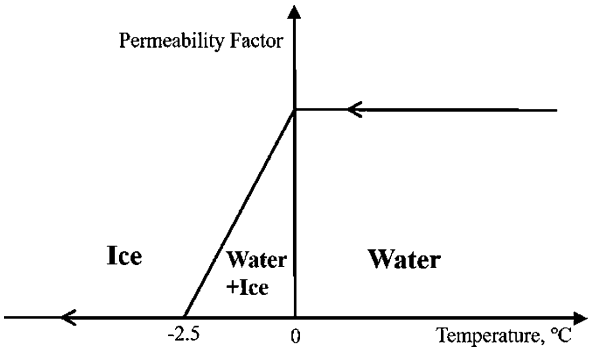

Fig. 12.10 Phase change of water (Shen 2014)

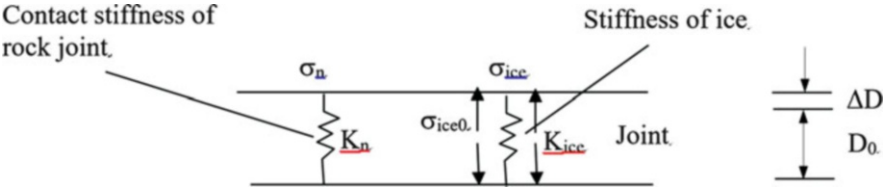

Fig. 12.11 Joint under ice swelling pressure (Shen 2014)

The swelling pressure due to the phase change of water depends on the modulus of the ice and rock. It has been reported that Young's modulus of ice at −10 °C is in the range of 9.7–11.2 GPa (Petrovic 2003). To simplify the process of modeling the ice ring, we consider only two phases: liquid phase and solid phase, and the phase change occurs at 0 °C temperature.

In a rock joint, the joint may be loaded by two types of forces (Fig. 12.11): Contact stress on the joint surface (σ_n), which is determined by the joint contact stiffness K_n and joint deformation. Swelling pressure from ice (σ_{ice}), which is a function of ice stiffness and joint deformability. Please refer to the previous study (Shen 2014) for the calculation process of the ice swelling pressure in a rock joint. This process has been implemented in FRACOD to simulate the ice swelling effect. It needs to be emphasized that the swelling effect should not be directly applied as a constant swelling pressure to the joint surface without considering the stiffness of the ice layer, because the initial swelling pressure will decrease rapidly when the rock joint starts to deform.

12.6 Thermal-Mechanical Coupling Function in FRACOD

The numerical model, including input data, boundary conditions, and initial conditions were constructed according to the previous test and modeling work (KIGAM 2003, 2004, 2005, 2006; Jung et al. 2012; Park et al. 2007a, b; Park et al. 2010). The temperature dependent strength parameters were used for accounting the tensile strength increase in cooling conditions. The initial temperature of the model was set 18 °C and −196 °C temperature boundary condition was applied on the cavern periphery and the 18 °C temperature boundary condition was applied on the surface boundary. Figure 12.12 shows the FRACOD model and the inner containment system of storage cavern.

The thermal-mechanical behavior of the concrete lining and surrounding rock after storing LN2 for 25 weeks was simulated and the results were compared with the field data. The following summarizes the results of case studies on the thermal-mechanical coupling in FRACOD.

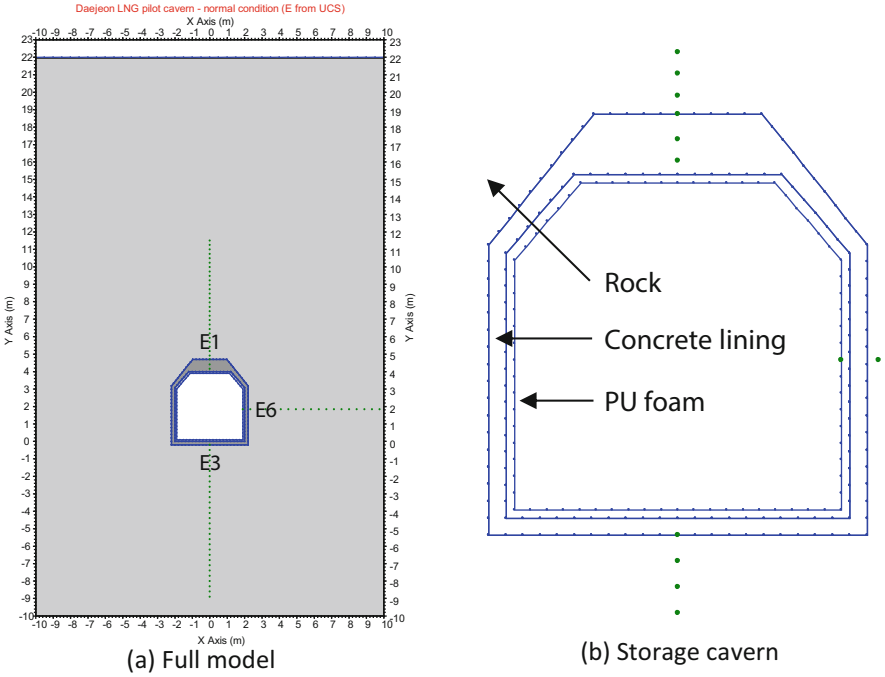

Fig. 12.12 FRACOD model of the pilot LNG storage cavern with monitoring positions of extensometers E1, E3 and E6 and the containment system of storage cavern. (Jung et al. 2014)

12.6.1 Case-I: Young's Modulus from the Compressive Test

At first, Young's modulus used in the Case-I was obtained from uniaxial compressive test and adjustment to the rock mass scale by using RMR. Total 15 thermal time steps were used for modeling 25 weeks because FRACOD has a limit of a maximum number of time steps. After 5-week cooling, the model didn't converge and failed to yield the results. The distribution of temperature and fracture initiation and propagation after 5-week cooling were shown in Fig. 12.13. The simulation result shows that despite the thermal insulation system, the concrete lining and rock mass are severely damaged and are not consistent with the field observations. The reason for such an analysis error may be a relatively high thermal stress and a large thermal time steps.

12.6.2 Case-II: Reduced Young's Modulus

While investigating the reasons for the excessive damage than the field observation, Young's modulus was considered as the main factor of high thermal stress. Thermal stress is basically dependent on the coefficient of thermal expansion, Young's modulus and the temperature difference including boundary conditions. Heating generally causes compressive thermal stresses while cooling results in tensile stresses. The Young's modulus of rocks is usually determined by uniaxial

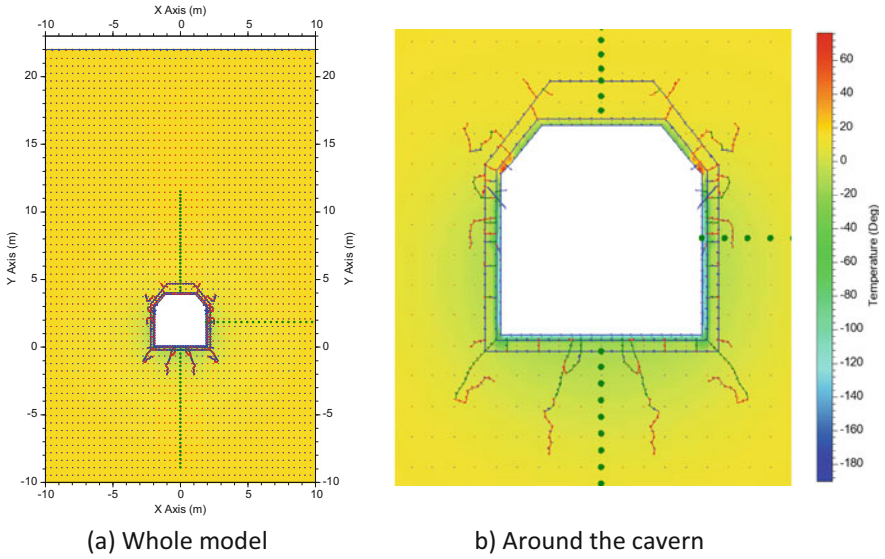

Fig. 12.13 The distribution of temperature and newly generated fractures around the pilot LNG storage caverns after 5-week cooling. This model showed error after this thermal time step

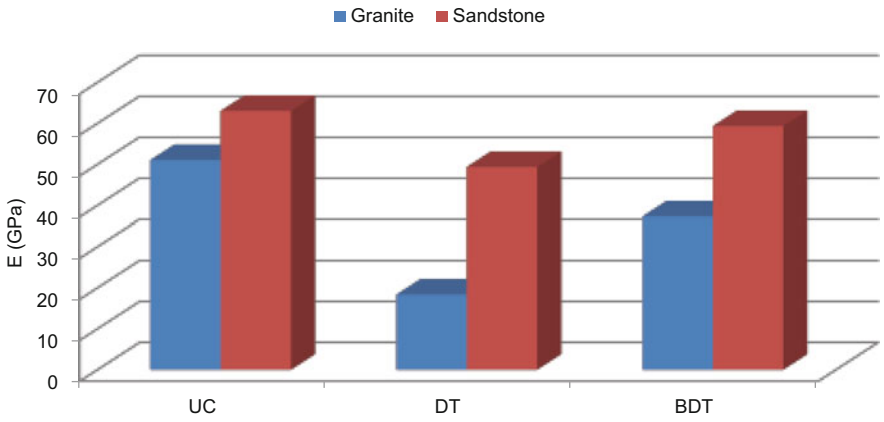

Fig. 12.14 Comparison of Young's modulus of two types of rocks under different loading conditions. (After Jung 2000). *UC* uniaxial compression, *DT* direct tension, *BDT* Brazilian disk test

compressive test. The Young's modulus from tensile tests showed the reduced value compared to that from the compressive test (Sundarm and Corrales 1980; Stimpson and Chen 1993; Chen and Stimpson 1993; Jung 2000). Based on the granitic host rock type and the results of Jung (2000) shown in Fig. 12.14, Only Young's modulus was reduced to 40% of Case-I and all other input values and conditions remained the same as Case-I.

The fracture initiated around the corner of the cavern and propagated through the rock mass, but the number of fractures was dramatically decreased in Case-II model as shown in Fig. 12.15. Cracks initiated in lining after 2-week cooling then propagated to the rock mass after 8-week cooling.

The distribution of temperature, minor principal stress and displacement are shown in Fig. 12.16. The effect of 25-week cooling was limited to the cavern periphery due to the lining and insulation system.

12.6.3 Comparisons with Field Data

The results of the Case-II model were compared with the monitored data during the operation of the pilot LNG storage cavern and showed good agreement. Comparison of the top region, Extensometer E1, was omitted because the application of convective thermal boundary condition above the liquid level is not possible under the current version of the code.

Figure 12.17 shows the temperature change obtained from the simulation along with the field data. As can be seen in Fig. 12.17, the numerical model yielded reliable results. In the case of displacement (Fig. 12.18), the trend was similar to each other although the magnitude of them showed a remarkable difference.

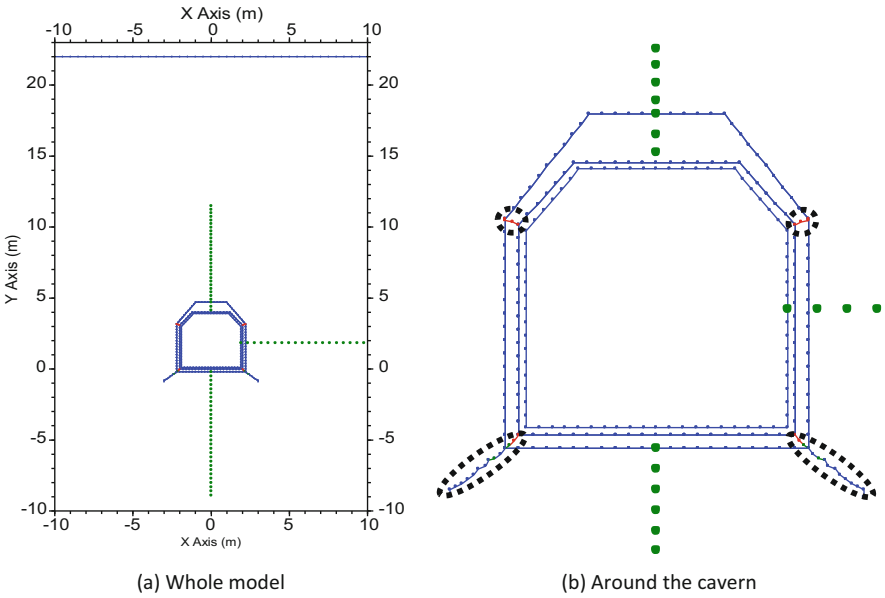

Fig. 12.15 Fracture initiation and propagation in case of reduced Young's modulus. The red and blue line in the dotted circle represents the opening and elastic fracture, respectively. Green dots represent monitoring points of temperature and displacement by extensometers

Thermal tensile stresses were developed as the zero isotherms propagated in the rock mass as shown in Fig. 12.19. Only the numerical results were shown in Fig. 12.19 for the lack of reliable field stress data. The results of displacement and stresses showed transition zone in the rock mass between expansion and shrinkage behavior. Then, tensile (shrinkage) region became dominant as the cooling effect propagated in the rock mass.

After the operation of the pilot LNG storage cavern, two horizontal and five vertical boreholes were drilled in the bottom and sidewall to investigate the integrity of the lining system and rock mass. The drilled core showed the complete bond between rock and concrete lining and the geophysical logging of drilled boreholes didn't detect any visible cracks. Also, the changes in the uniaxial compressive strength of rock and concrete before and after operation were examined, but there was little difference.

12.7 Discussions

Case-I numerical model showed larger damaged region by many thermal cracks and was not consistent with the results of the field survey. While Case-II model considering reduced Young's modulus showed only one or two thermal cracks around the

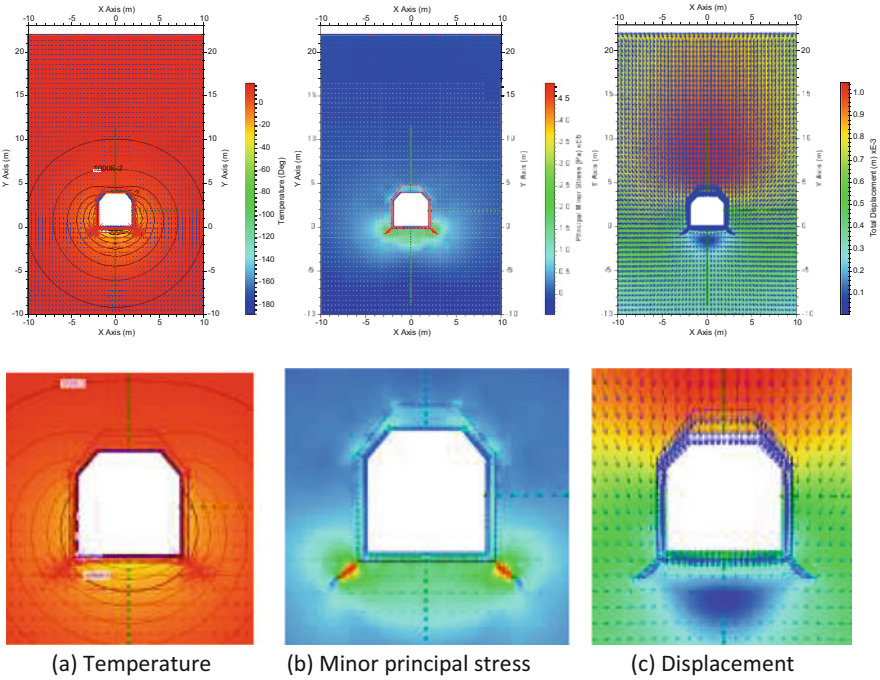

Fig. 12.16 The distribution of simulation results in the case of reduced Young's modulus

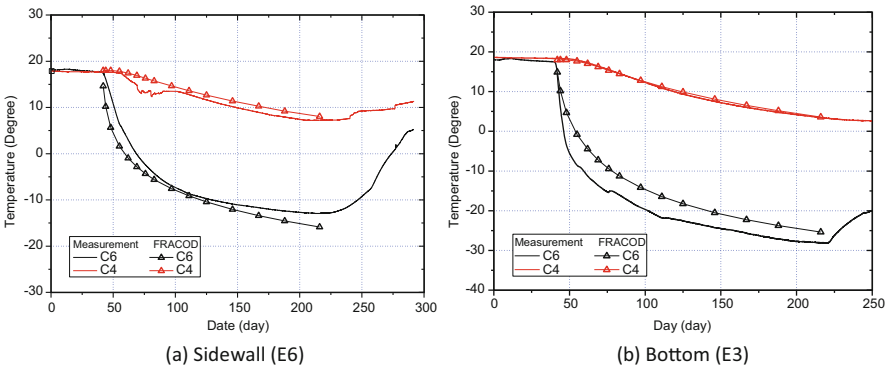

Fig. 12.17 Comparison of the temperature changes obtained from numerical analysis and measurements during the operation of the pilot LNG storage cavern

corner of the cavern due to the stress concentration by the sharp geometry, which is well matched with the field data.

Cooling generally yields tensile stress because the cooled material shrinks as the temperature drops. In addition, Young's modulus, which plays an important role in estimating the thermal-mechanical behavior of the rock mass is usually smaller in

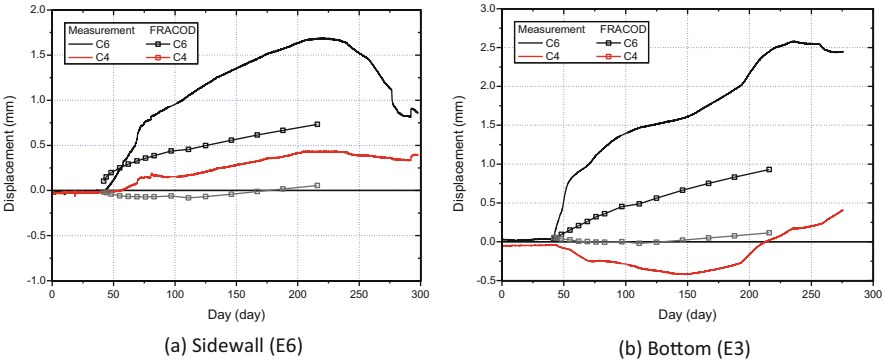

Fig. 12.18 Comparison of the displacement trend obtained from numerical analysis and measurements during the operation of the pilot LNG storage cavern

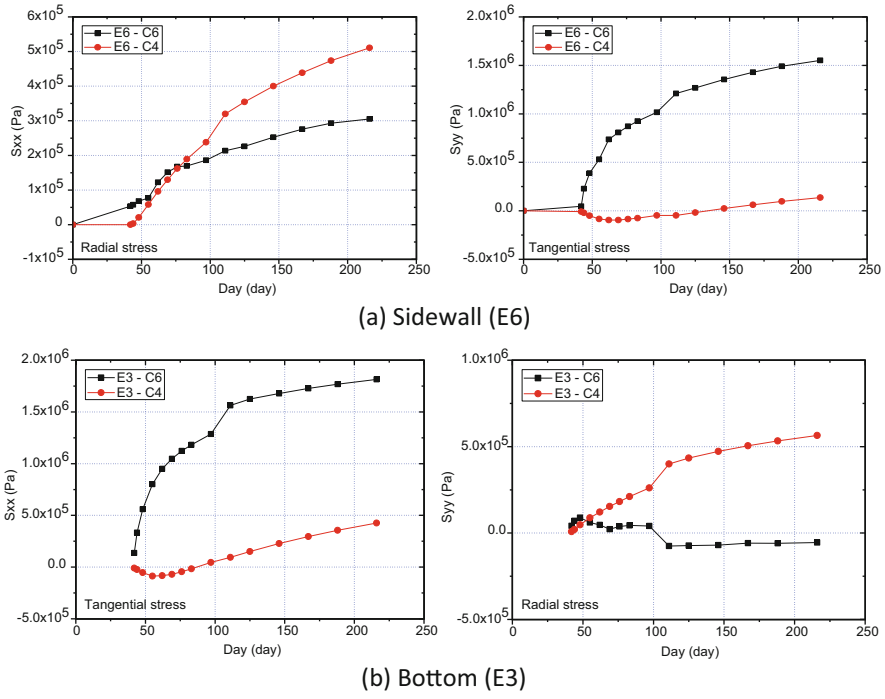

Fig. 12.19 Change of radial and tangential stress during the cooling operation

tensile mode than the compressive mode. Consequently, the use of Young's modulus obtained from a compressive test would overestimate thermal stresses in case of cooling. It is recommended that Young's modulus obtained from a tensile test should be used for the accurate and reliable estimation of thermal stress under cooling conditions.

Also, the discrepancy between the measured and predicted values in the displacement may be due to various causes, but the main reason is that the volumetric expansion of the water-ice phase change is not considered and the discontinuous rock mass is regarded as a continuous material. In FRACOD development, how to include these functions will be very meaningful and useful for evaluating the T–H–M coupled behavior of the rock mass during underground cryogenic storage. Although the fully coupled T-H-M model of the discontinuous rock mass can be a better solution, the effectiveness and efficiency of using the complex model should be investigated.

12.7.1 Ice Swelling Function in FRACOD

During this numerical study, different models are used as shown in Fig. 12.20. The first model in Fig. 12.20(a) is similar to that used by Jung et al. (2014) and the surrounding rock mass is treated as a homogeneous, isotropic and elastic medium. The rock mass is assumed to be impermeable and non-porous in FRACOD due to the code limitation. A previous study (Jung et al. 2014) using this model has found that only limited fracture propagation occurred at the bottom corners during the cooling stage due to high tensile stress concentration.

In the second model, we have introduced cracks with random orientations in the vicinity of the LNG cavern. These cracks are assumed to have a hydraulic aperture that enables them to hold water. The water may then become ice if the local

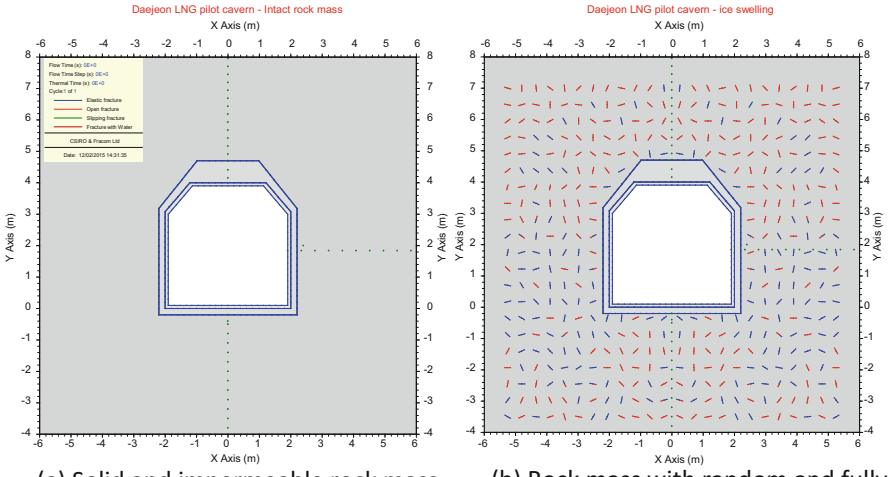

Fig. 12.20 FRACOD models used for investigating the effect of ice swelling in the pilot LNG cavern experiment (Shen et al. 2015)

temperature drops below zero and creates swelling pressure in the rock mass. In theory, these cracks serve the same purposes as the pores and microcracks in the rock mass if they are small and dense enough. However, due to the limitation in modeling capacity, it is impossible to use the actual sizes of the microcracks and pores.

Hence as a simplification, we used cracks with a length of approximately 20 cm and a density of 4 cracks per square meter. Each crack has a hydraulic aperture of 6.25 mm, 12.5 mm, and 37.5 mm respectively in three simulation cases. The volume of water held in these cracks is equivalent to that stored in the pores of the host rock mass with a porosity of 0.5%, 1%, and 3% respectively. Note that the hydraulic aperture is often different from the mechanical aperture in the real world because the hydraulic aperture is strongly affected by the connectivity of the voids. In this study, the hydraulic aperture is fairly high in order to simulate the water storage in the pores, and it has no direct connection with the mechanical aperture.

The mechanical and thermal properties of the rock and lining materials are used in the previous study (Shen et al. 2015). Note that Young's modulus of the rock and concrete lining used in this study represents the lower end of a range of measurement results using different methods, and it also considers the scale effect from laboratory scale to field scales. Of those geotechnical monitoring instruments, Extensometer E6 into the sidewall of cavern and Extensometer E4 into the floor are of particular interests of this study.

Using these models, the following five different cases as are designed to investigate the effects of random cracks and ice swelling on the displacement and stresses in the surrounding rock mass:

Case 1: Pure thermo-mechanical model where the rock mass is treated as an impermeable medium and no ice formation is considered.
Case 2: Thermal-mechanical model with dry cracks in the rock mass and no ice formation.
Case 3: Thermal-mechanical model with saturated cracks and possible ice formation in the surrounding rock mass. In this case, Young's modulus of ice is assumed to be 10 GPa and the volume expansion factor from water to ice is 0.09. Crack hydraulic aperture is 5.8 mm, which has a water holding capacity equivalent to a rock mass with a porosity of 0.5%;
Case 4: Same as Case 3 except the equivalent rock porosity is 1.0%;
Case 5: Same as Case 3 except the equivalent rock porosity is 3.0%.

12.7.2 Temperature

The modeled temperature distribution after 28 days, 84 days and 175 days of cooling are shown in Fig. 12.21. The area of rock temperature below zero has been grown significantly during this period from the immediate floor and sidewalls to a distance of about 2 m into the rock mass. This is the area where ice can form and potentially cause swelling pressure.

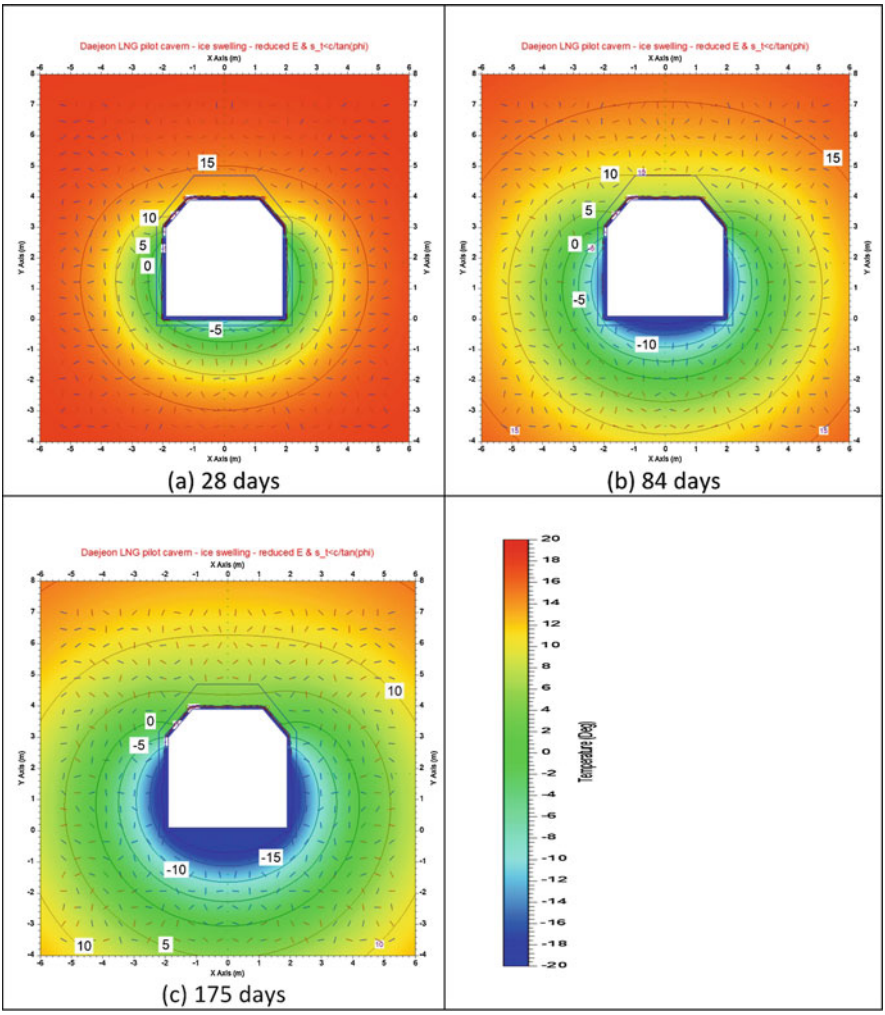

Fig. 12.21 Modeled temperature distribution in the rock mass around the cavern

The modeled temperature change has been compared with the measurement results at four locations on the sidewalls and floor (Fig. 12.22). The four locations include two at a distance of 0.5 m into the sidewall (Extensometer E6 anchor C6) and floor (Extensometer E4 anchor C6), and two at the distance of 4.3 m into the sidewall (Extensometer E6 anchor C4) and floor (Extensometer E4 anchor C4).

Overall, the modeled temperature change and the measured results agree well, indicating the thermal evolution of the models is sufficient. Note that the two models with and without cracks give the exactly the same temperature results as the thermal effects of the cracks are ignored during the modeling.

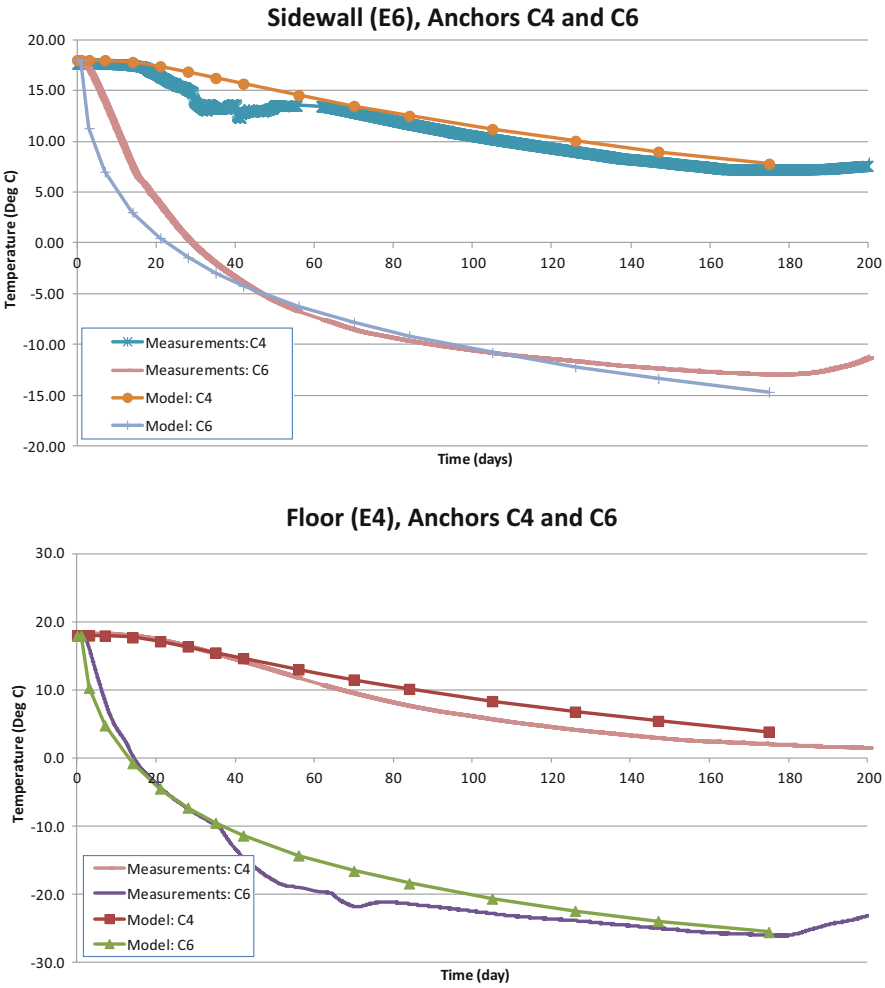

Fig. 12.22 Comparison of modeled and measured temperature change at different monitoring locations in the sidewall and floor of the pilot LNG cavern

12.7.3 Displacement

The displacement of rock mass around the cavern during the cooling stage depends on many factors such as temperature change, rock mechanical properties (e.g. Young's modulus), rock mass thermal expansion factor, and the effect of ice swelling. The measured relative displacement of the rock mass within 4 m from the cavern wall and floor (anchors C4 and C6 in both extensometers E6 and E4) showed a maximum of 1.8 mm and 2.8 mm, both being rock mass shrinkage (Fig. 12.23). It is understood that this shrinkage was caused by the cooling of the rock mass.

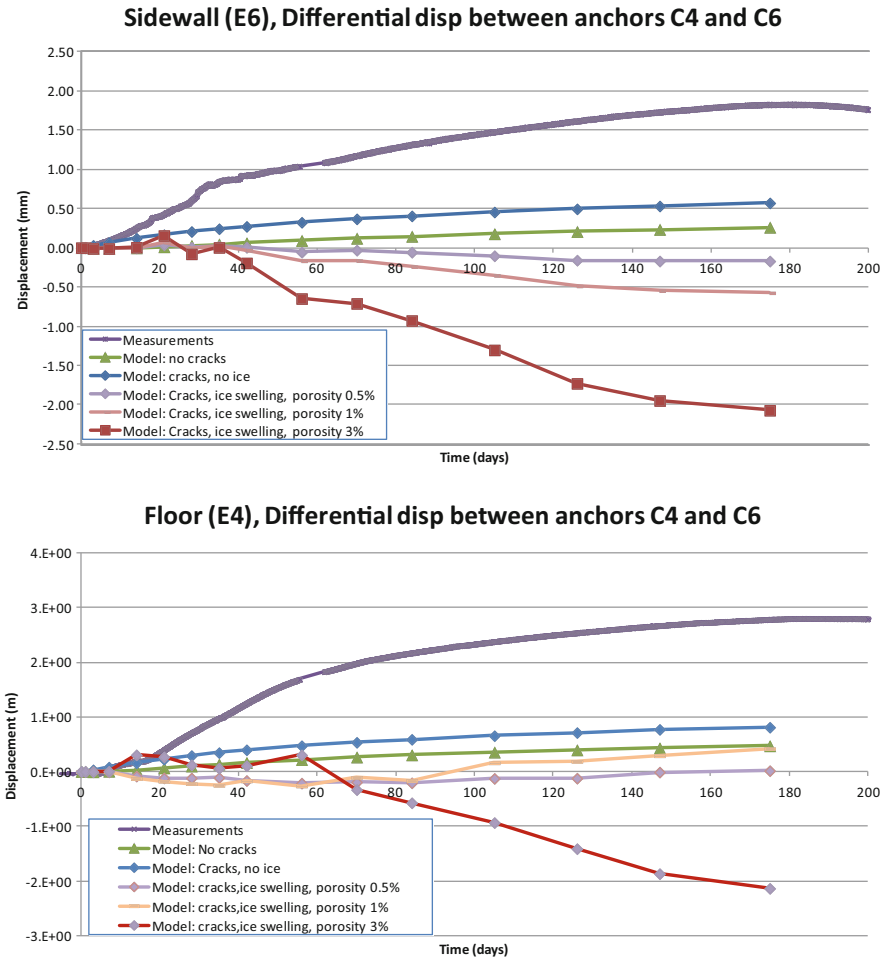

Fig. 12.23 Comparison between the modeled and measured differential displacements in the sidewall and floor

For the five cases modeled using FRACOD, the predicted relative displacements between anchors C4 and C6 in both the side wall and the floor are also shown in Fig. 12.23.

In Cases 1 and 2, which did not consider the expansion due to freezing, the direction of the predicted relative displacement between C4 and C6 was similar as shrinkage of rock mass due to cooling, although the magnitude and slope of the predicted displacement showed a relatively large difference compared to the measured value. This phenomenon has previously been found by Jung et al. (2014) and briefly discussed. Uncertainty in rock thermo-mechanical properties used in the models and possibly in the measurement data could have contributed to the mismatch between the measured and predicted results.

As can be seen in Fig. 12.23, when the ice swelling is considered in the model with random cracks, the predicted differential displacement in sidewall became negative which indicates a net expansion of the rock mass. With the equivalent rock porosity of 0.5%, the predicted maximum expansion displacement is 0.16 mm. This displacement is increased to 0.6 mm and 2.1 mm after 175 days when the equivalent rock mass porosity is 1% and 3%, respectively. A similar trend is observed for the predicted displacement in the floor where the maximum expansion displacement is 2.1 mm after 175 days for an equivalent rock mass porosity of 3%. With a lower porosity of 0.5% and 1%, the displacement curves with time seem to be more complex as they are initially expansion (negative) and later become shrinkage (positive). This may reflect the complex behavior of the rock mass with randomly distributed cracks.

Figure 12.24 shows the modeled normal displacements of the random cracks in the surrounding rock mass for Case 3 (porosity = 0.5%). All saturated cracks within the frozen region of the rock mass have crack opening displacement due to ice swelling. The maximum normal displacement is about 0.8 mm.

The ice swelling has made the predicted displacement further departing from the measured displacement with extensometers. If the measured displacement is indeed shrinkage as reported rather than expansion, the enlarged mismatch between measured and predicted displacements when ice swelling is considered may suggest that at the pilot LNG site the ice formation in the surrounding rock mass is very limited.

Nevertheless, the modeling results in Fig. 12.24 indicate the potential impact of the ice swelling. As the granite rock porosity is mostly in the range of 0.5–1.5% and it will be higher if discontinuities such as cracks and joints in rock mass are considered, the effect of ice swelling can be more significant. It will more than compensate for the thermal shrinkage caused by the cooling effect and cause rock mass expansion. Consequently, it will change the stress state in the rock mass and has an important implication on the permeability of the rock mass.

12.7.4 Stresses

The effect of ice swelling can further be demonstrated by examining the stress distribution in the surrounding rock mass, see Fig. 12.25. Without random cracks and ice formation, the stresses in the vicinity of the pilot LNG cavern are predominately tensile stresses, induced by the cooling of the rock (Fig. 12.25(a)). The introduction of random cracks in the surrounding rock mass has somehow altered the tensile stress distribution as the cracks open under tension which consequently releases the tensile stresses (Fig. 12.25(b)). When ice swelling is considered, the stresses in the frozen region of the surrounding rock mass are pre-dominantly compressive stresses (Fig. 12.25(c)–(e)).

The overall areas with compressive stress increase with the rock mass porosity, so as the average magnitude of compressive stresses. At a porosity of 3%, the compressive stress in the frozen region reached more than 10 MPa, only localized tensile

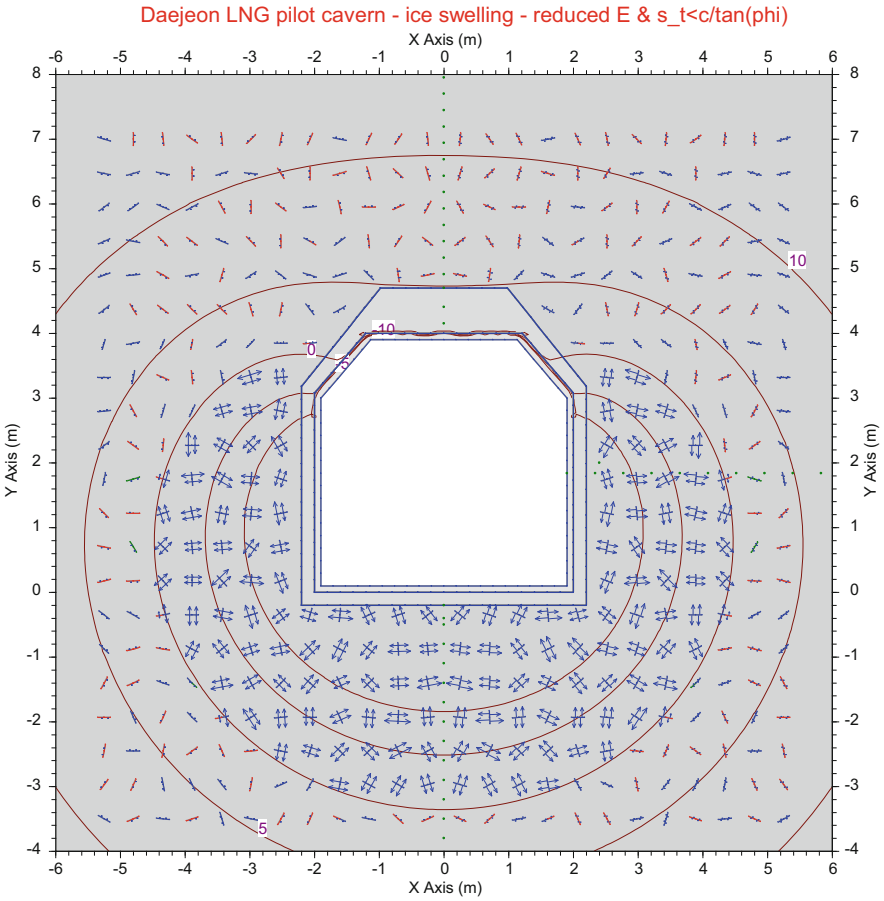

Fig. 12.24 Crack normal displacement due to ice swelling (porosity = 0.5%) in regions with sub-zero temperature after 175 days. The temperature distribution is indicated by the contours and the crack normal displacement is plotted as a vector

stresses exist due to the crack tip effect. The compressive stress is expected because the ice formation in the random cracks increases the overall volume of the rock matrix, which more than compensates the rock mass shrinkage due to thermal effect. As a result, the rock mass is compressed and hence thermal induced tensile stress diminishes and compressive stress is increased.

Figure 12.26 shows the variation of tangential stress in the sidewall and floor for different cases with and without ice swelling.

Without ice swelling, the tangential stress in both locations is tensile stress and its maximum magnitude of about 2 MPa after 175 days. With ice swelling, the tangential stress at the two locations becomes compressive stress, and its magnitude increases with the equivalent porosity used in the model. It reaches as high as 23 MPa in the sidewall and 16 MPa in the floor for a rock mass porosity of 3%.

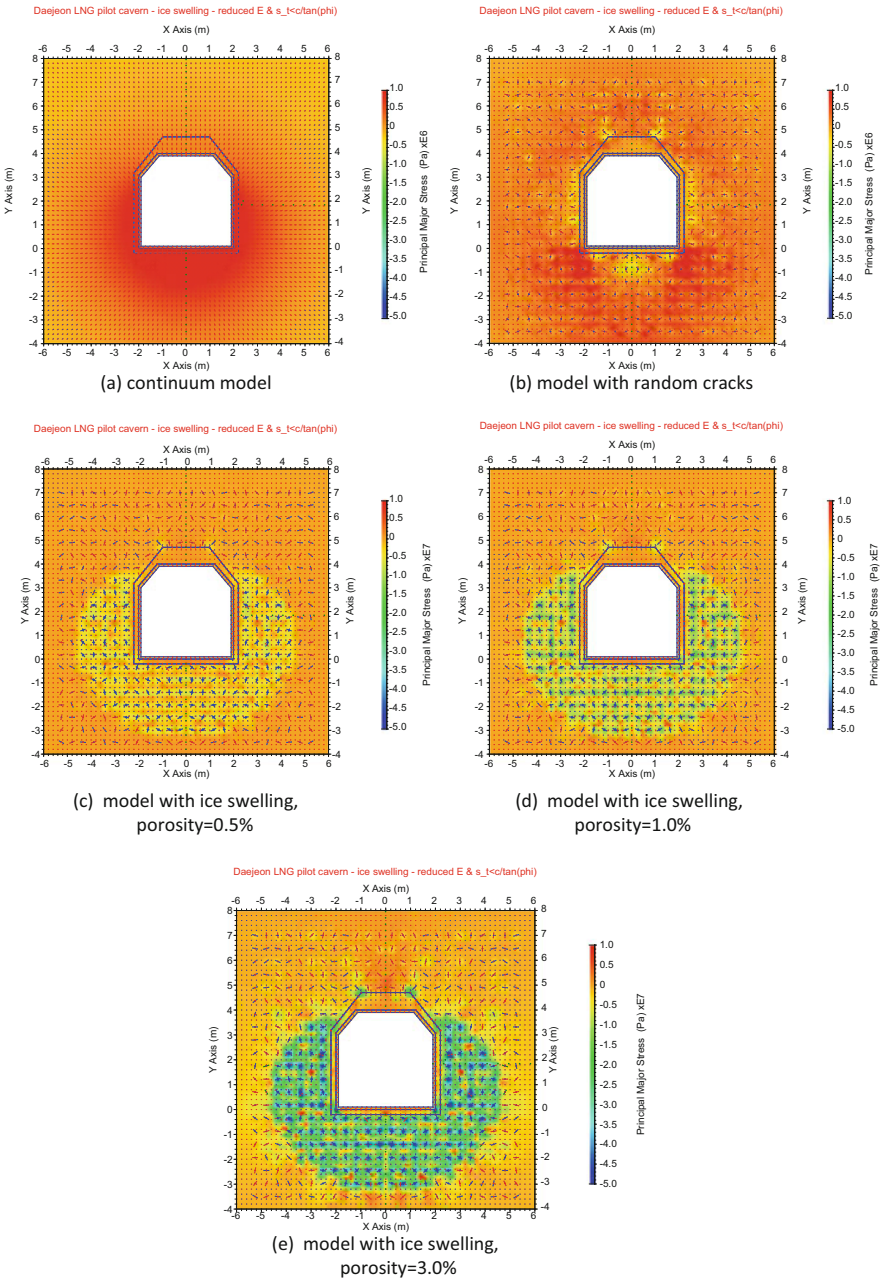

Fig. 12.25 Major principal stress distribution in surrounding rock mass after 175 days of cooling

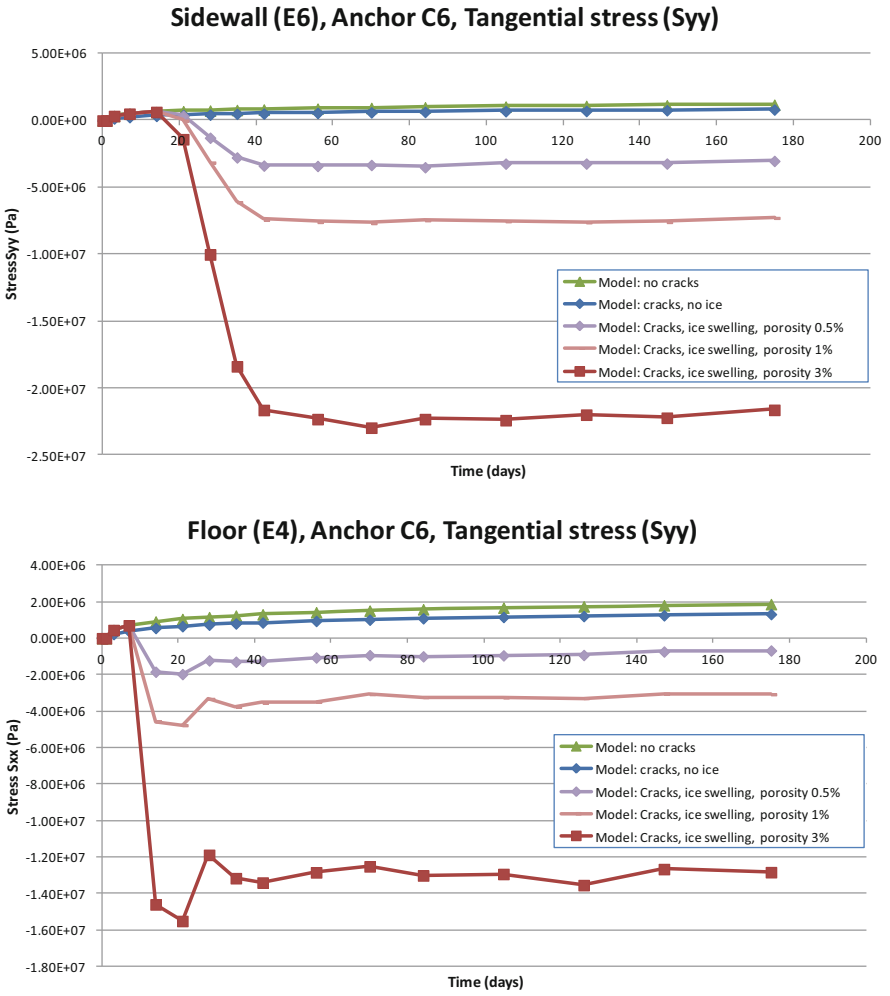

Fig. 12.26 Tangential stress in the sidewall and the floor at the location of anchor C6 of both extensometers E6 and E4

The change from tensile zone to the compression zone in the surrounding rock mass due to ice formation has important implications for the integrity of the LNG cavern. With ice formation, the voids in the rock mass will be sealed and the permeability of the rock mass will be significantly reduced, which prevents LNG seepage into the rock. The compressive stresses in the immediate vicinity of the cavern will make it impossible for tensile cracks to initiate and propagate, and hence limit the possibility of LNG leakage into the rock mass through fracture channels.

This study is based on the assumption that the pores and cracks in the surrounding rock mass are fully saturated during the cooling stage. In reality, the surrounding rock mass of an underground LNG cavern is likely to be dewatered initially during

the construction stage. Water may flow back once the cavern is in operation with LNG. It is commonly expected that ice ring will form where the groundwater meets the zero temperature fronts. However, this does not mean that the ice will not be formed in the area much closer to the cavern. The dewatering measures are normally effective to drain the free water in the rock matrix but ineffective to remove the water trapped in pores and isolated cracks. Therefore, ice formation and swelling pressures will still be able to occur in dewatered zones.

12.7.5 Conclusions

FRACOD is a modeling package designed to simulate complex rock fracturing processes. With the support from an international collaboration project where CSIRO, SKEC, and KIGAM are all the principal partners, FRACOD has recently been advanced to consider coupled thermal-hydro-mechanical processes and it also includes a new function to consider ice swelling.

In order to simulate the fracture initiation and propagation of thermal fractures around the pilot LNG storage cavern, thermal-mechanical coupled analyses have been carried out using FRACOD and the capability of the code has been verified by a comparison of numerical results with *in situ* measurement data. Original model, Case-I overestimated thermal tensile stress and damaged zone compared with the field data. Temperature and fracture initiations were well matched with the field data in case of reduced Young's modulus (Case-II) was used.

In the case of displacement, the magnitude and slope of the predicted displacement are relatively large compared to the measured ones, although the prediction direction is similar. This was partially attributed to the volume expansion during the water-ice phase change because this model didn't consider this phenomenon. According to the numerical analyses in which the estimated stress was significantly overestimated than the observation in the field, the different behavior under heating and cooling conditions must be considered for the appropriate modeling of the thermal-mechanical coupled problems. More specifically, Young's modulus obtained from the tensile test should be used in case of cooling environments.

Also, the results from this study including ice swelling function have demonstrated that the ice swelling in the surrounding rock mass of the pilot LNG cavern can play a major role in rock mass displacement and rock stresses. Without considering ice swelling, the predicted rock displacements are shrinkage. Whereas when the ice swelling is considered the predicted rock displacements become expansion. This result clearly shows that ice swelling is a key contributing factor in the rock mass response to LNG storage. Also noticed in this study is that, with ice formation and swelling pressure, the stresses in the immediate vicinity of the pilot LNG cavern is compressive. This means that tensile fracturing in this region is unlikely and the chance of LNG leakage into the rock mass is low. This new understanding is a significant improvement to the conventional thinking that tensile fracturing may occur in the rock walls due to thermal effect from LNG storage.

In conclusion, FRACOD has been demonstrated in this study to be effective in modeling the LNG underground storage cavern. And the introduction of random saturated cracks is an effective way to directly model the ice formation and ice swelling pressure.

Future work in this area should be focused on increasing the FRACOD capability which enables us to use very fine microcracks in the numerical model. It will make the model closer to reality and the results can then be refined. It is also envisaged that this modeling approach will be applied to the actual full-scale LNG underground storage cases whenever such cases are available.

References

Amantini E, Chanfreau E (2004) Development and construction of a pilot lined cavern for LNG underground storage. In: 14th international conferences and exhibition on liquefied natural gas, Doha, Qatar. PO-33

Amantini E, Chanfreau E, Kim HY (2005) The LNG storage in lined rock cavern: pilot cavern project in Daejeon, South Korea. In: Proceedings, GASTECH 2005: 21st international conference and exhibition for the LNG. LPG and Natural Gas Industries, Bilbao, pp 1–16

Broms L, Fredriksson A, Glamheden R, Pilebro H (2001) Conversion of an oil storage cavern to a refrigerated LPG storage facility. Eurock 2001, Espoo

Cha SS, Lee JY, Lee DH, Amatini E, Lee KK (2006) Engineering characterization of hydraulic properties in a pilot rock cavern for underground LNG storage. Eng Geol 84:229–243

Cha SS, Lee KK, Bae GO, Lee DH, Gatelier N (2007) Analysis of rock drainage and cooling experiments for underground cryogenic LNG storage. Eng Geol 93:117–129

Chen R, Stimpson B (1993) Interpretation of indirect tensile strength tests when moduli of deformation in compression and in tension are different. Rock Mech Rock Eng 26(2):183–189

Chung S K (2006) Thermo-mechanical behavior of rock masses around underground LNG storage cavern. In: Keynote lectures in Rock Mechanics in Underground Construction – 4th Asian Rock Mechanics Symposium, Singapore, pp 19–28

Glamheden R (2001) Thermo-mechanical behaviour of refrigerated caverns in hard-rock. Thesis for the degree of Doctor of Philosophy, Chalmers University of Technology, Göteborg, Sweden

Goodall D C (1989) Prospects for LNG storage in unlined caverns. In: Proceedings of the international conference on storage of gases in rock caverns, Trondheim, Balkema, pp 237–243

Jacobsson U (1977) Storage of liquefied gases in unlined refrigerated rock cavern. In: Proceedings of the first international symposium on storage in excavated rock caverns, Stockholm

Jung Y B (2000) Deformation and failure characteristics of rocks under low temperature. Ph.D. thesis, Seoul National University, Seoul, Korea

Jung YB, Park ES, Chung SK, Kim HY (2011) Coupled hydro-thermal modeling of ice ring formation around a pilot LNG cavern in rock. Eng Geol 118:122–133

Jung YB, Park ES, Shen B (2014) Thermal–mechanical analysis of the fracture initiation and propagation around the underground pilot LNG storage cavern. Geosyst Eng 17(6):331–341

KIGAM (2003) Development of base technology for underground LNG storage and the analysis on the operation results of pilot plant. 147p (in Korean)

KIGAM (2004) Development of base technology for underground LNG storage and the analysis on the operation results of pilot plant—2004. 144p (in Korean)

KIGAM (2005) Development of base technology for underground LNG storage and the analysis on the operation results of pilot plant—2005. 123p (in Korean)

KIGAM (2006) Development of base technology for underground LNG storage and the analysis on the operation results of pilot plant—2006. 177p (in Korean)

Kim H Y (2006) 25 Years' experience of underground hydrocarbon storage in Korea and over-stresses problems in large rock cavern. Invited Lecture 2006 handouts, Japan Society of Civil Engineers, pp 1–27

Kim JH, Park SG, Yi MJ, Son JS, Cho SJ (2007) Borehole radar investigations for locating ice ring formed by cryogenic condition in an underground cavern. J Appl Geophys 62:204–214

Kovári K (1993) Basic consideration on storage of compressed natural gas in rock chambers. Rock Mech Rock Eng 26(1):1–27

Lasseter TJ, Witherspoon PA (1974) Underground storage of liquified natural gas in cavities created by nuclear explosives. Lawrence Livermore Laboratory, University of California, Berkeley

Lee D H, Kim H Y, Gatelier N, Amantini E (2003) Numerical study on the estimation of the temperature profile and thermo-mechanical behaviour in rock around the Taejon LNG pilot cavern. In: International symposium on the fusion technology of geosystem engineering, rock engineering and geophysical exploration, Seoul, Korea, pp 233–237

Lee HS, Lee DH, Kim HY, Choi YT (2006) Design criteria for thermo-mechanical stability of rock mass around lined rock cavern for underground LNG storage. Tunn Undergr Space Technol 21:337

Park E S (2006) Thermo-mechanical consideration for the cryogenic storage. In: International workshop on the Underground Storage Facilities in conjunction with the 4th ARMS, Singapore, pp. 81–98

Park ES, Chung SK, Lee DH, Kim HY (2007a) Experience of operating an underground LNG storage pilot cavern. In: 11th ACUUS conference, Athens, Greece, pp 157–162

Park ES, Chung SK, Lee HS, Lee DH, Kim HY (2007b) Design and operation of a pilot plant for underground LNG storage. In: Eberhardt E, Stead D, Morrison T (eds) Proceedings of 1st Canada–US rock mechanics symposium. Taylor & Francis, Vancouver, pp 1221–1226

Park ES, Jung YB, Song WK, Lee DH, Chung SK (2010) Pilot study on the underground lined rock cavern for LNG storage. Eng Geol 116:44–52

Park ES, Chung SK, Kim HY, Lee DH (2011) The new way to store LNG in lined rock caverns. In: The 2011 World Congress on Advances in Structural Engineering and Mechanics (ASEM'11), Seoul, pp 3951–3956

Petrovic JJ (2003) Review mechanical properties of ice and snow. J Mater Sci 38:1–6

Rahman MK, Hossain MM, Rahman SS (2000) An analytical method for mixed-mode propagation of pressurized fractures in remotely compressed rocks. Int J Fract 103:243–258

Shen B (2014) Development and applications of rock fracture mechanics modelling with FRACOD: a general review. Geosyst Eng 17:235–252

Shen B, Jung YB, Park ES, Kim TK (2015) Modelling the effect of ice swelling in the rock mass around an LNG underground storage cavern using FRACOD. Geosyst Eng 18(4):181–198

Stimpson B, Chen R (1993) Measurement of rock elastic moduli in tension and in compression and its practical significance. Can Geotech J 30:338–347

Sundaram PJ, Corrales JM (1980) Brazilian tensile strength of rocks with different elastic properties in tension and compression. Int J Rock Mech Min Sci 17:131–133

Yi MJ, Kim JH, Park SG, Son JS (2005) Investigation of ground condition change due to cryogenic conditions in an underground LNG pilot plant. Explor Geophys 36:67–72